Modal Parameter Estimation in Transmissibility Functions from Digital Image Correlation Measurements

Ángel J. Molina-Viedma[1](✉), Manuel Pastor-Cintas[1], Luis Felipe-Sesé[1], Elías López-Alba[2], José M. Vasco-Olmo[2], and Francisco Díaz[2]

[1] Departamento de Ingeniería Mecánica y Minera, Campus Científico Tecnológico de Linares, Universidad de Jaén, 23700 Linares, Spain
ajmolina@ujaen.es

[2] Departamento de Ingeniería Mecánica y Minera, Campus Las Lagunillas, Universidad de Jaén, 23071 Jaén, Spain

Abstract. High-speed digital image correlation is a camera-based displacement measurement technique that has experienced increasing popularity for modal analysis. It is due to a high spatial density of measurement that provides an outstanding interpretation of mode shapes or operational deflection shapes. However, its sensitivity is typically lower than other techniques and transducers such as accelerometers or laser vibrometry. With these measurements, the estimation of any transfer function in the frequency domain is noisier in valley regions of the response, including anti-resonances. Therefore, an accurate analytical model of the response should be used for modal identification. Modal analysis algorithms perform an identification of the modal parameters and a reconstruction of the response based on the transfer function between force excitation and displacement response. This is called the frequency response function. However, force measurements are not available in many experiments, where the motion excitation is recorded instead. This is the case when the vibration is applied to the specimen through a motion in its base. This transfer function, also known as the transmissibility function, relates the motion of excitation and response, whose shape differs from the frequency response function. This difference in the response function is relevant in a relatively noisy measurement like using digital image correlation. Hence, in this work, a transformation of the transmissibility function into equivalent frequency response function, based on theoretical models, is performed prior to modal identification in base motion tests. More suitable experimental response functions are obtained, increasing the accurateness of the modal parameter estimation.

Keywords: Modal analysis · Transmissibility functions · Full-field measurement

1 Introduction

In recent years, optical techniques have attracted the attention of the scientific community in vibration and modal analysis thanks to the development of high-speed cameras

Z. Dimitrovová et al. (Eds.): WMVC 2022, MMS 125, pp. 799–806, 2023.
https://doi.org/10.1007/978-3-031-15758-5_82

technology. The main advantage of these novel methodologies is that they perform contactless measurement without modifying the mechanical behavior of the system. With an appropriate image processing, full-field measurements are obtained. This represents an extremely high-density grid of virtual sensors, i.e., measurement points. Hence, useful data can be obtained with vision techniques which provide both alternative and complementary tools in modal analysis [1], quite useful for model updating [2].

One of the most used techniques is Digital Image Correlation (DIC). This technique has been widely employed for dynamic studies and also in the field of modal analysis. It has been employed for modal identification using both simplified single-degree-of-freedom [3] and multi-degree-of-freedom methods [4–6], and also for operational modal analysis [7, 8]. The modal identification algorithms are based in frequency response functions (FRF) [9], a transfer function between the displacement response and the force excitation. However, in many experimental situations is not possible to perform and measure pointwise forces to obtain FRFs at different coordinates. Applying a motion excitation in the base or support of the structure is one of the most common alternatives to force excitation. Hence, the vibration is transmitted from the base to the system and, now, the transfer function relates the motion of the measured degrees-of-freedom (DOF) of the structure and the motion of the base. This is known as the transmissibility function and its theoretical expression differs from the FRF's. Hence, using conventional identification without a convenient transformation of the data may entail erroneous modal parameter estimation [10].

This work evaluates modal identification on transmissibility functions where the full-field response is measured by 3D-DIC under base motion excitation. A transformation of the transmissibility functions is accomplished to suit classical identification procedure based on frequency response functions fitting [10, 11]. The comparison with the original transmissibility functions, as measured in the test, reveals how the obtained modal model fits better the experimental behaviour, especially concerning mode shapes and curve synthesis.

2 Base Excitation for Modal Analysis

When a mechanical system is subjected to motion excitation in its support, z, the governing equations for a system excited through the base are condensed in this matrix equation [10]:

$$[M]\{\ddot{x}\} + [C]\{\dot{x}\} + [K]\{x\} = -\ddot{z}\{g\}[M] \tag{1}$$

where [M], [C], [K] are the mass, damping, stiffness matrices [g] is a vector function of the geometry. The damping and stiffness forces, which depend on the relative motion between adjacent DOF, x, are defined by relative coordinates to the base frame as the base motion is a common term in the absolute motion of all the DOF. Conversely, inertial forces depend on the absolute motion, $\{\ddot{x}\} + \ddot{z}\{g\}$. However, it has been organized so that the left side of Eq. (1) is expressed in terms of the relative coordinates. Moreover, the right side is only function of the excitation.

On the other hand, when force excitation is applied at a certain coordinate, the transfer function between force magnitude, F, and displacement magnitude, X, depending on the harmonic term, ω, is known as frequency response function, $[H]$:

$$\{X\} = [H]\{F\} \tag{2}$$

This relation is the basis for experimental modal analysis, where FRFs are experimentally measured through the frequency-domain signals of displacements and loads.

In the base motion configuration, if the excitation is harmonic, the magnitude of the equivalent force can be expressed as:

$$\{F\} = -\ddot{Z}\{g\}[M] \tag{3}$$

and, therefore,

$$\{X\} = -[H]\{g\}[M]\ddot{Z} \tag{4}$$

Comparing Eqs. (2) and (4) and being $\{g\}$ and $[M]$ constant, it is found out that an FRF relating X and F is proportionally equivalent to the transmissibility function, $-[H]\{g\}[M]$, between the relative motion to the base, X, and the magnitude of the base motion acceleration, $\ddot{Z}$. Therefore, transmissibility functions in this form can be employed as regular FRFs in modal analysis.

3 Experimental Procedure

When base excitation is put into practice and DIC is employed to measure the response, the response coordinates are usually measured in terms of absolute motion. The aim of this work is to reveal the errors committed during the modal characterization in absolute response transmissibility functions using FRF-based identification algorithms. To carry out this, modal analyses for those transmissibility functions and those defined in terms of relative motion, equivalent to FRFs, were compared through modal parameters and synthesized response curves reconstruction.

In this study, a rectangular polycarbonate plate with dimensions 210 mm in length, 140 mm in width and 4 mm in thickness was designed through a modal analysis in a finite element model to contain several modes in a frequency range suitable for DIC. Experimentally, the plate was fixed at its central point to a shaker, through a rigid joint, as shown in Fig. 1 (a).

In this test, a random excitation signal was applied from 20–500 Hz. The base excitation was registered by an accelerometer placed on the shaker's armature. The response was recorded by a stereoscopic system consisting of two high-speed cameras (FastCam SA4 from Photron, 50 mm lenses, 1 megapixel) was employed. A schematic layout of the setup is shown in Fig. 1. The recording frame rate was 1000 fps. In total, two sequences of 5457 images each were recorded. A DAQ system (NI USB-6251 DAQ) was devoted to acquiring the accelerometer signal, synchronised with the high-speed cameras.

A commercial DIC algorithm was used (VIC-3D software by Correlated Solutions Inc) in order to process the images. This technique performs tracking of subsets of

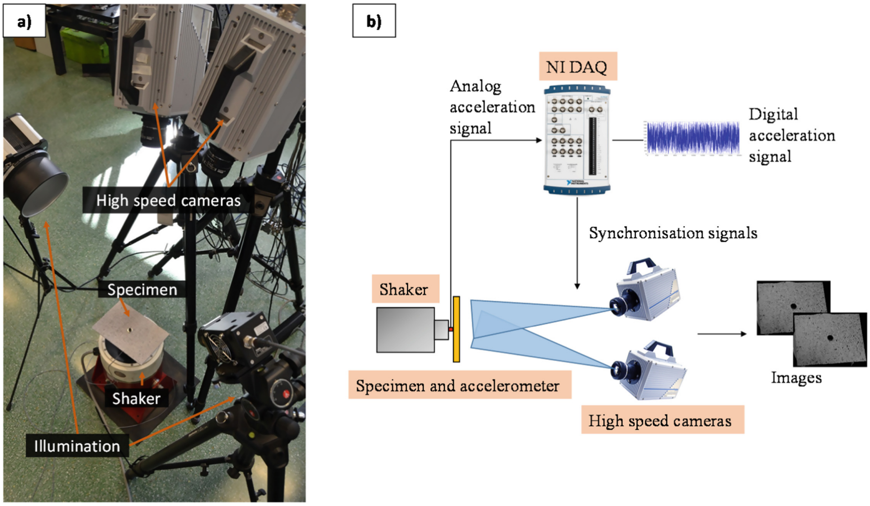

Fig. 1. (a) Picture and (b) scheme of the experimental set up.

the region of interest based on correlation criteria. For this purpose, a habitual procedure of specimen preparation was carried out, consisting in covering with a white paint background and, afterwards, adding black dots to make a random speckle pattern.

Afterwards, both the absolute and relative motion transmissibility functions were estimated and employed as input data for the characterisation of modal parameters using FRF-based method. Particularly, a standard identification method was considered in this study, the least-squares complex exponential (LSCE) [9].

At the first stage, the poles of the system, which contain the natural frequency and damping of the physical modes, were identified through the stability diagram.

Once the poles were extracted, a linear least-squares frequency-domain solver is used to obtain the residues in Eq. (1) by fitting the curve to the given experimental transmissibility functions. In this step, mode shapes are defined. In addition to the identification of the modal parameters, the synthetised transmissibility reconstruction was assessed.

4 Results

In view of the above, the absolute and the relative motion transmissibility functions were obtained. The first step of the analysis is the poles identification using a LSCE procedure. Maximum order of 15 was chosen to evaluate the stability of poles, avoiding the over-fitting of computational poles.

The resulting stability diagrams for each assumption are shown in Fig. 2. Three resonances can be visually identified in the average function from each data set. Preliminarily, certain differences are observed in the curves, more evident in the low-response regions between resonance peaks. It includes the low-frequency spectrum before the first resonance, which reveals the raising trend toward 0 Hz in the original transmissibility function, as a false pole. With both transmissibility functions sets, the three modes are quickly stabilized at a model order of about six using the identification algorithm. No great differences were found in the poles values between the relative motion data and the absolute one. It can be observed in the resulting natural frequency and damping ratio values, in Table 1.

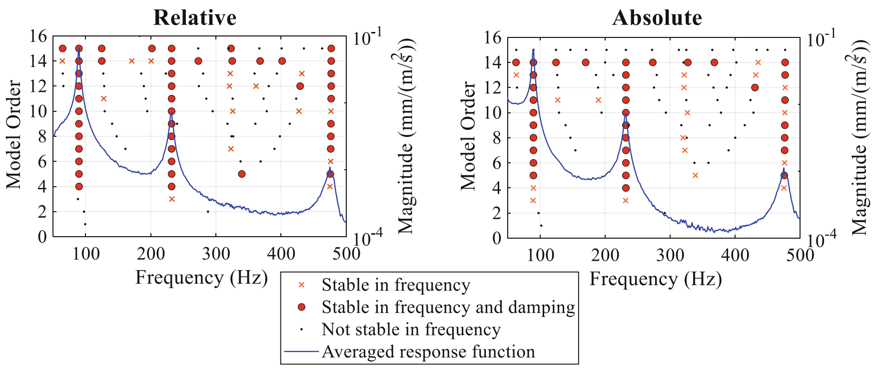

Fig. 2. Stabilisation diagrams for the relative and absolute motion transmissibility functions.

Table 1. Natural frequencies and damping ratios for the relative and absolute motion transmissibility functions.

	Natural freq. (Hz)		Damping ratio	
	Rel. motion	Abs. motion	Rel. motion	Abs. motion
Mode 1	89.616	89.666	1.30	1.31
Mode 2	231.579	231.576	1.01	1.01
Mode 3	475.331	475.387	1.02	0.99

Subsequently, using the identified poles, mode shapes could be obtained. The resulting maps are shown in Fig. 3, for each case, using amplitude normalization. As opposed to the natural frequencies and damping ratios, they show clearer differences between datasets. Despite the fact that there are differences in the first and second modes, the third mode, with its more complex and stiffer shape, exposes more clearly the differences between the original and adapted functions. This differences appear as an overestimation of the amplitude in the out-of-phase regions.

This observation can be confirmed by the curve synthesis analysis. In Fig. 4, the synthesized response curves of two points are depicted along with the experimental curves. One point is located at the corner, where a high response is expected in most of the modes. The second one is placed in the middle of the right half of the plate. It can be observed that the low-response areas are poorly fitted in the original data. For instance, the adapted data have allowed for a better fitting of the low-frequency spectrum, below the first mode. Moreover, it provided the appropriate representation of the anti-resonance before the second mode at the corner point. Furthermore, false

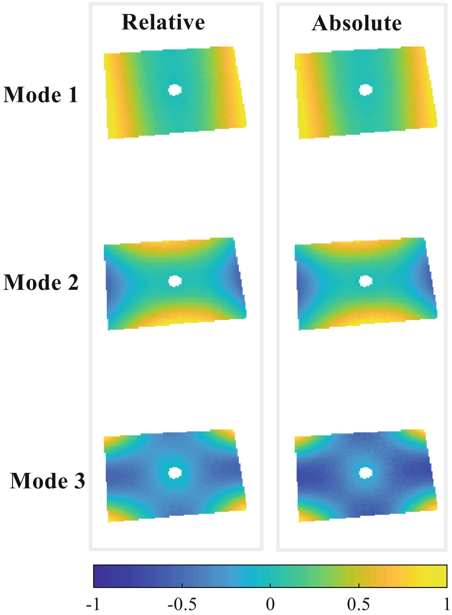

Fig. 3. Modal shapes obtained for the relative and absolute motion transmissibility functions.

anti-resonances are described by the synthesized curve for the original data around the third resonance peak. Besides these deficiencies, remarkable behavior is presented in the second plotted point regarding the third mode fitting. Whereas the peak amplitude is properly described for the adapted data, the estimation of the third mode amplitude in the original data is noticeable higher than experimental. This point is located in the region where the highest differences between the third mode estimation take place, according to Fig. 3. Therefore, it reveals the overestimation of amplitude in the third mode in these regions due to the non-suitable shape of the original curves for the FRF-based procedure.

Another indicator of the accuracy of the curve fitting is the error. In the corner point the minimum error is observed for both data set: 1.2% and 2.3% for the relative motion and absolute motion data. In the corners the higher displacement amplitudes are obtained and the committed error is low. Conversely, the error increases as approaching the fixation, where the lower displacements appear. The error in the second depicted point in Fig. 4 is 8,2% for the relative motion data whereas it reaches the 21,7% for the absolute motion data, up to 86% error in the fixation surroundings.

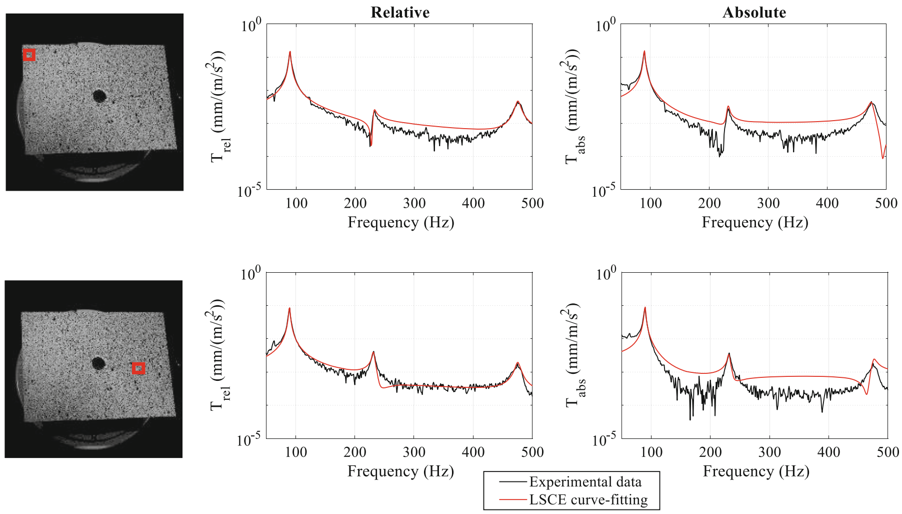

Fig. 4. Curve synthesis at two measurement points for the relative and absolute motion transmissibility functions.

5 Conclusions

This work addresses the analysis of the validity of the FRF-based algorithm for modal estimation for base excitation tests using DIC. It is motivated by the increasing popularity of vision techniques for their contactless full-field measurements. Moreover, base motion excitation is quite common in practice and requires specific treatment for the analysis.

3D-DIC was employed for the experimental test in order to determine the full-field response of a plate. The convenient transformation of the transmissibility functions from absolute to relative response terms was performed to be employed for FRF-based identification methods. Namely, modal analysis was carried out applying one of the best-known modal identification procedure. The benefits of the transformation are not totally revealed in the natural frequencies and damping ratios estimation, as no major differences were found, but in the mode shapes estimation and the curve synthesis. The comparison of the mode shapes, enhanced by the full-field information of DIC, showed discrepancies in amplitude for the absolute response transmissibility functions. It was definitively confirmed by the analysis of the synthesized curves synthesis, where the error in the fitting procedure was found to be significantly higher for the absolute response transmissibility functions. This remarks the necessity of adapting the experimental data to obtain accurate modal models using FRF-based identification procedures.

References

1. Baqersad, J., Poozesh, P., Niezrecki, C., Avitabile, P.: Photogrammetry and optical methods in structural dynamics – a review. Mech. Syst. Signal Process, **86**, 17–34 (2017)
2. Wang, W., Mottershead, J.E., Ihle, A., Siebert, T., Reinhard Schubach, H.: Finite element model updating from full-field vibration measurement using digital image correlation. J. Sound Vib. **330**, 1599–620 (2011)

3. Trebuňa, F., Hagara, M.: Experimental modal analysis performed by high-speed digital image correlation system. Measurement **50**, 78–85 (2014)
4. Molina-Viedma, Á.J., Felipe-Sesé, L., López-Alba, E., Díaz, F.A.: Comparative of conventional and alternative digital image correlation techniques for 3D modal characterisation. Meas. J. Int. Meas. Confed. **151**, 107101 (2020)
5. Huňady, R., Hagara, M.: A new procedure of modal parameter estimation for high-speed digital image correlation. Mech. Syst. Signal Process **93**, 66–79 (2017)
6. Zanarini, A.: Full field optical measurements in experimental modal analysis and mod-el updating. J. Sound Vib. **442**, 817–42 (2019)
7. Chang, Y.-H., Wang, W., Chang, J.-Y., Mottershead, J.E.: Compressed sensing for OMA using full-field vibration images. Mech. Syst. Signal Process **129**, 394–406 (2019)
8. Uehara, D., Sirohi, J.: Full-field optical deformation measurement and operational modal analysis of a flexible rotor blade. Mech. Syst. Signal Process **133**, 106265 (2019)
9. Ewins, D.J.: Modal Testing: Theory, Practice, and Application, 2nd edn. Research Studies Press LTD., Baldock (2000)
10. Béliveau, J.G., Vigneron, F.R., Soucy, Y., Draisey, S.: Modal parameter estimation from base excitation. J. Sound Vib. **107**, 435–49 (1986)
11. Molina-Viedma, Á.J., Felipe-Sesé, L., Pastor-Cintas, M., López-Alba, E., Díaz, F.A.: Evaluation of modal identification under base motion excitation using vision techniques. Mech. Syst. Signal Process **179**, 109405 (2022)